Astronomy & Astrophysics manuscript no. paper˙feh˙testv9.1
July 25, 2011

Metallicity of M dwarfs

II. A comparative study of photometric metallicity scales⋆

V. Neves[1,2,3], X. Bonfils[2], N. C. Santos[1,3], X. Delfosse[2], T. Forveille[2], F. Allard[4], C. Natário[5,6], C. S. Fernandes[5], and S. Udry[7]

[1] Centro de Astrofísica, Universidade do Porto, Rua das Estrelas, 4150-762 Porto, Portugal
email: vasco.neves@astro.ua.pt
[2] UJF-Grenoble 1 / CNRS-INSU, Institut de Planétologie et d'Astrophysique de Grenoble (IPAG) UMR 5274, Grenoble, F-38041, France.
[3] Departamento de Física e Astronomia, Faculdade de Ciências, Universidade do Porto, Portugal
[4] Centre de Recherche Astrophysique de Lyon, UMR 5574: CNRS, Université de Lyon, École Normale Supérieure de Lyon, 46 Allée d'Italie, F-69364 Lyon Cedex 07, France
[5] Centro de Astronomia e Astrofísica da Universidade de Lisboa, Campo Grande, Ed. C8 1749-016 Lisboa, Portugal
[6] Leiden Observatory, Leiden University, The Netherlands
[7] Observatoire de Genève, Université de Genève, 51 Chemin des Maillettes, 1290 Sauverny, Switzerland

Received XXX; accepted XXX

ABSTRACT

We present a comparative test of several photometric metallicity calibrations of M dwarfs proposed in the literature. Our test sample is made of 23 M dwarfs, companion of widely separated (> 5 arcsec) F-, G- or K- dwarfs with known or newly measured uniform metallicities. We include M dwarfs with reliable V photometry by restricting our sample to stars with V uncertainty lower than ∼0.03 dex. Among all calibrations, we find that the one of Schlaufman & Laughlin (2010) provides lower offset and residuals against our sample and, ultimately, we used our larger sample to update and marginally improve their calibration. Despite better V photometry than used in previous studies, the dispersion remains largely in excess given the [Fe/H] and photometric uncertainties. This suggests the remaining dispersion has physical rather than experimental roots.

Key words. stars: abundances – stars: fundamental parameters – stars: planetary systems – stars: late type stars: atmospheres

1. Introduction

Most recently, increased interest in M dwarfs has come from planet search programs. Putative planets induce larger reflex velocities and transit depths when they orbit and transit M dwarfs, compared to FGK stars. Lower mass, smaller and possibly habitable planets are therefore easier to find around them, and are indeed detected at an increasing pace (Udry et al. 2007; Mayor et al. 2009).

From the ever growing number of exoplanets, interesting statistical properties emerge from their characteristics or the characteristics of their host stars (e.g. Udry & Santos 2007; Bonfils et al. 2011, in prep.). Among those, the planet-metallicity correlation is one of the most remarkable : stars with higher metal content have, on average, a higher probability to host Jovian planets (Gonzalez 1997; Santos et al. 2001, 2004; Fischer & Valenti 2005). Within the core-accretion paradigm of the planetary formation, that property is expected to extend to the cooler M dwarfs: to counterbalance the lower mass of their protoplanetary disks, and provide enough material to form a planet of similar mass, their density has to increase. And, while the planet-metallicity correlation seems to vanish for FGK stars that host Neptunes and lower-mass planets (Sousa et al. 2008; Bouchy et al. 2009), it might remain persistent for M dwarfs that host Neptune-mass planet [ref].

Probing the planet-metallicity correlation for M dwarfs has largely motivated the first metallicity calibration (Bonfils et al. 2005), but only two M-dwarf hosts were known at the time. A few more planet detections later on allowed the comparison of the metallicity distributions of M dwarfs *with* and *without* known planets, finding that they have a ∼ 11% probability of being drawn from the same parent distribution (Bonfils et al. 2007). Today, even

⋆ Based on observations collected with the FEROS, ELODIE and SOPHIE spectrographs under the programs 060.A-9120(B), 073.D-0802(A), 074.D-0670(A)

after more planets have been detected, and the calibration improved, the probability that M-dwarf hosts are more metal rich than the common M dwarf is evaluated to be $\sim 6\%$ (Schlaufman & Laughlin 2010). Although this result lines with the core accretion paradigm, the confidence level of that difference remains below 3 σ. Multiplying the number of known planets and improving metallicity determinations further are therefore the two avenues that must be pursued to better measure the correlation between the stellar metallicity and the planet occurrence for M dwarfs.

However, the measurement of the stellar parameters of M dwarfs from their spectra is not a trivial task. As the stellar subtype increases, the number of diatomic and triatomic molecules (e.g. TiO, VO, H_2O, CO, etc) in their atmospheres increases, effectively depressing the continuum and making a line-by-line spectroscopic analysis impossible for all but the earlier subtypes. These complex features are not fully reproduced by atmospheric models, themselves limited by incomplete opacity databases. In this context, several techniques, more or less successful, have been employed to measure the metal content of M dwarfs [ref].

We aim to test recently published photometric calibrations of the M-dwarf metallicity. To that purpose, we have built a comparison sample of 23 M dwarfs with accurate photometry and parallaxes (Sect. 2). Then, we propose a test to compare different calibrations (Sect. 3) and choose to review, compare and discuss three works on the subject (Sect. 4). Those works are Bonfils et al. (2005), Johnson & Apps (2009) and Schlaufman & Laughlin (2010), and we refer to them as B05, JA09 and SL10, respectively. Actually, two expressions are proposed in B05, one that calibrates metallicity in a color-magnitude diagram, which is commonly used in the literature, and a second that calibrates metallicity as a function of a mass anomaly. We wish to have both expressions in our comparison list and refer to them as B05 and B05(2), respectively. We also sieze the opportunity of an increased sample to update the metallicity calibration of SL10 and thus add this fifth calibration to our list. Note that for completeness, we also consider the works of Casagrande et al. (2008) and Rojas-Ayala et al. (2010) but defer their description to an appendix, the former because it does not exactly qualify as a calibration (it requires input from an existing calibration and do not provide an expression), the later because it goes beyond the photometric calibrations of our paper by bringing metallicity scale to a higher spectral resolution. Finally, Sect. 5 presents our conclusions.

2. Sample and Observations

We aim to test different calibrations and, much like most calibrations discussed in this paper, we make use of FGK+M binaries. The metal content is determined on the primaries with classical techniques and assumed to be the same for the secondaries. Our first step is therefore to build a sample of such binaries.

Our selection was made using the catalog of nearby stars (Gliese & Jahreiß 1991), the catalog of nearby wide binary and multiple systems (Poveda et al. 1994), the catalog of common proper-motion companions to *Hipparcos* stars (Gould & Chanamé 2004), and the catalog of disk and halo binaries from the revised Luyten catalog (Chanamé & Gould 2004). To avoid light cross-contamination when recording spectra we chose systems with wide separations only (> 5 arcsec). Quality photometry has been a concern and thought to limit former calibrations. When we picked V photometry from the literature, we therefore applied a strict threshold and dismissed stars with photometry no better than 0.03 dex. Mermilliod et al. (1997) has been our main source of Johnson-Cousins VRI photometry for the secondaries. The JHK_S photometry was taken from 2MASS (Skrutskie et al. 2006) except in the case of Gl 551 (Bessell 1991). For 10 sources RI photometry was in Weistrop and Kron systems instead of Johnson-Cousins. We therefore applied transformations following Weistrop (1975) and Leggett (1992), respectively. The parallaxes are those of the primaries and were taken from the revised *Hipparcos* catalog (van Leeuwen 2007). Care was taken not to include fast rotators, spectroscopic binaries, and stars without (matching) common proper motions.

Our final sample is composed of 19 M-dwarf secondaries and extend slightly to the K-dwarf domain with 4 additional K7/K8 secondaries. Actually, the selection described above lead to a much larger sample of almost 300 binaries. Of which, only a small part has been observed and reduced. The most important factors in the selection of the sample is the lack of precise metallicity and parallax measurements for the primary, precise photometry for the secondary, and proper motions for the pair at the same time.

The metallicity of the primaries were either computed from their spectra or taken from the literature. For 9 stars we obtained spectra with the spectrograph FEROS installed on the 2.2m ESO/MPI telescope in La Silla (Kaufer & Pasquini 1998). We followed the procedure described in Santos et al. (2004) and determined [Fe/H] by imposing excitation and ionization equilibrium. In those cases the Fe lines were measured using the program ARES (Sousa et al. 2007) with the Fe line list of Sousa et al. (2007). A grid of Kurucz model atmospheres (Kurucz 1993) is also used in this process, as well as the radiative transfer program MOOG (Sneden 1973). The parameters that were determined by this method are described in Table 1.

For 3 stars, we used spectra gathered with the CORALIE and SOPHIE spectrographs (Queloz et al. 2000; Bouchy et al. 2006), and determined their metallicity from a calibration based on the cross correlation function (CCF) of their spectra and numerical templates, following Santos et al. (2002). The CCF method was used due to the fact that the CORALIE and SOPHIE spectra are too contaminated with the light of the ThAr lamp (used for high-precision RV measurements) to properly derive the stellar parameters. This method can be used on con-

Table 1. Stellar parameters measured from the primaries. The [Fe/H] of the M dwarf secondary is inferred from the primary.

Primary	Secondary	T_{eff} [K]	log g [dex]	v_t [dex]	[Fe/H] [dex]
Gl100A	Gl100C	4804 ± 81	4.82 ± 0.24	1.25 ± 0.24	-0.28 ± 0.03
Gl105A	Gl105B	4910 ± 65	4.55 ± 0.14	0.77 ± 0.18	-0.19 ± 0.04
Gl157A	Gl157B	4854 ± 71	4.75 ± 0.19	1.31 ± 0.20	-0.16 ± 0.03
Gl173.1A	Gl173.1B	4888 ± 72	4.72 ± 0.16	0.97 ± 0.21	-0.34 ± 0.03
Gl231.1A	Gl231.1B	5951 ± 14	4.40 ± 0.03	1.19 ± 0.01	-0.01 ± 0.01
Gl297.2A	Gl297.2B	6461 ± 14	4.65 ± 0.02	1.74 ± 0.01	0.03 ± 0.05
Gl559A	Gl551	5857 ± 24	4.38 ± 0.04	1.19 ± 0.03	0.23 ± 0.02
Gl666A	Gl666B	5274 ± 26	4.47 ± 0.04	0.74 ± 0.05	-0.34 ± 0.02
NLTT34353	NLTT34357	5489 ± 19	4.46 ± 0.03	0.91 ± 0.03	-0.18 ± 0.01

taminated spectra because the effect of the contamination is the same for all lines and all spectra and, as the CCF method is a calibration, its zero point is adjusted in the end to give the correct result.

From the literature, we picked 6 determinations from Bonfils et al. (2005) and 4 from Sousa et al. (2008), both of which used the same method as described in Santos et al. (2004)[1]. We also took one [Fe/H] value from Valenti & Fischer (2005) obtained with full spectral synthesis technique. As shown in Sousa et al. (2008), all the sources of stellar [Fe/H] have values that are in the same scale, with non-significant offsets.

The full references for all parameters are listed in Table A.3 in the Appendix.

3. A test for the calibrations

With a sample of M dwarfs with known metallicity we can test the different calibrations. To assess their respective quality, we measure the offset and the variance between observed and predicted values for each calibration.

As suggested in previous works (Schlaufman & Laughlin 2010; Rojas-Ayala et al. 2010), we also measure the residual mean square RMS_p (a variance normalized by the number of free parameters), and the multiple correlation coefficient R^2_{ap}, as described by Hocking (1976). The RMS_p is defined as

$$RMS_p = \frac{SSE_p}{n-p}, \qquad SSE_p = \sum (y_{i,model} - y_i)^2, \qquad (1)$$

where SSE_p is the residual sum of squares for a p-term model, n is the number of data points, and p is the number of free parameters. The R^2_{ap} is defined as

$$R^2_{ap} = 1 - (n-1)\frac{RMS_p}{SST}, \qquad SST = \sum (y_i - \bar{y})^2. \qquad (2)$$

A lower value of RMS_p means that the model being tested is best suited for prediction, while a R^2_{ap} closer to 1 signifies that the tested model explains most of the variance of the data. Negative values are allowed for R^2_{ap} and imply that the model being tested increases the variance compared to a constant model.

[1] this determination was actually done by the same team.

We note that when a fit is performed, p is the number of adjusted parameters and that, conversely, when a previously adjusted model is evaluated against a new independent sample, no parameter needs to be adjusted ($p = 0$). In our case, 11, 2, and 12 M dwarfs are common to our sample and the samples used to derive the calibrations of Bonfils et al. (2005), Johnson & Apps (2009) and Schlaufman & Laughlin (2010), respectively. Our sample therefore is not fully independent from previous calibrations. Instead, each calibration partially fits our sample already. Hence p cannot be zero but should rather take a value between zero and the number of parameters that were free back when the calibrations were adjusted. Despite an uncertain p value we present the results for these tests and generally use $p = 0$. Only when we update the calibration of Schlaufman & Laughlin (2010) with our new sample we use $p = 2$.

Finally, to attribute uncertainties to the offset, dispersion, RMS_p, and R^2_{ap}, we used a bootstrap method. We generated 100,000 virtual samples with the same size of our observed sample. Each time, we draw random elements, with repetition, and computed the described parameters. In the end, we used the standard deviation of the quantities to estimate uncertainties.

Along the paper, we show the comparison between calibrations in Fig. 1 and place the results of our tests in Table 2.

Fig. 1 shows the plots of the [Fe/H] obtained from the calibrations versus the spectroscopic [Fe/H]. The black line depicts a one to one relationship. Below each plot is shown the metallicity difference between the calibrations and the spectroscopic values. The black dashed line is the zero point of the metallicity difference, and the red dotted line represents the average of the metallicity difference. Table 2 displays the different equations for each calibration, when relevant, as well as the offset of each calibration, the dispersion around the mean value (rms), the residual mean square (RMS_p), and the adjusted square of the multiple correlation coefficient (R^2_{ap}). Along with these quantities, the table presents their uncertainties.

Table 3 displays the metallicity values from spectroscopy and the different calibrations, where the individual values for each star can be directly compared.

The uncertainties calculated for the parameters, in Table 2, show that the rms values are the most robust, having small dispersion values. In particular, the R^2_{ap} uncertainties imply a large variation of this parameter when using different sub-samples. This may mean that this parameter is not well suited for explaining the goodness-of-fit of a model, at least for small samples.

4. The latest metallicity measurements and calibrations

4.1. Calibration of Bonfils et al. (2005)

Woolf & Wallerstein (2005) measured equivalent widths of atomic lines from high resolution spectra of 35 M and K dwarfs, as classically done for FGK dwarfs, but with updated atmospheric models. Faced by models' limitations, they apply this approach on the M dwarfs with the earliest ($T_{eff} > 3500$ K) and most metal-poor (median [Fe/H]$= -0.89$ dex) subtypes. They later extended the study to 32 additional stars (Woolf & Wallerstein 2006), and show that metallicity correlates with CaH and TiO molecular indices, without proposing a calibration though.

If the molecular bands render model-based techniques difficult, they have photometric effects that are nevertheless useful to retrieve the metallicity. Increased abundances in TiO and VO shift a large amount of flux from the visible (dominated by the opacities of these species) to the infrared (where the flux is re-radiated). For a given mass, the bolometric luminosity is concurrently diminished when the metallicity increases. Both effects work together in the visible and largely cancel in the infrared, such that the V magnitude is largely dependent on metallicity while infrared magnitudes are not (Chabrier & Baraffe 2000; Delfosse et al. 2000).

B05 used that effect as a metallicity scale, and to calibrate that scale, used binary (or multiple) stars with a FGK primary and a M dwarf secondary. The calibration is based on a $\{(V-K)-M_K\}$ color-magnitude diagram. The metallicity was measured on the primaries with a classical line-by-line analysis and assumed to be the same for the M-dwarf components. To make a larger sample, they pool their metallicity measurement with Woolf & Wallerstein (2005)'s determination and derived a calibration with a $\sim$0.2 dex dispersion. Then, they used the calibration to measure the metallicity distribution of a volume-limited sample of 47 M dwarfs and found them slightly metal poor compared to FGK stars (by 0.07 dex[2]), with a modest significance of 1.3 σ. After few more planets have been detected, and as already mentioned above, Bonfils et al. (2007) used the same calibration to compare M dwarfs with and without planets and found that planet hosts are marginally metal rich.

B05 and Bonfils et al. (2006) also examined the metallicity distribution of M dwarfs, without distinguishing planet hosts from single stars, and compared the distribution with FGK stars. Applying their calibration to a volume limited sample of 47 M dwarfs and comparing to 1,000 FGK stars from the CORALIE planet-search program, they found M dwarfs to be slightly metal poor by 0.07 dex, albeit with a confidence level of 2.6 σ only.

With this paper's sample, we measure that the B05 calibration has an offset of -0.05 ± 0.04 dex and a dispersion of 0.20$\pm$0.02 dex. Interestingly, correcting from that offset almost cancels the metallicity difference between M dwarfs and FGK stars. Naturally, it does not affect the possible metallicity difference between M dwarfs with and without known planets. The negative offset is in line with the result of SL10 (see Section 4.3) that B05 underestimates, in general, the true value of [Fe/H].

SL10 reports a R^2_{ap} value lower than 0.05 for the B05 calibration and stated that their model explains almost an order of magnitude more of the variance of the calibration sample. In Sect. 3, we noted, however, that the value of p is uncertain when there is an overlap between samples. Moreover, we compute large uncertainties for R^2_{ap} and point it is probably not a robust estimator. Against our sample, and using p=0, we find $R^2_{ap} = 0.32 \pm 0.16$ dex. That value is higher than reported by SL10 and tends, therefore, to mitigate the improvement from this calibration.Is this remark in the last phrase too strong? What is your opinion?

In addition to the commonly used calibration, B05 also provides another expression to evaluate [Fe/H]. That second expression, labeled B05(2) in Table 2, is based on the difference between the V- and K-band expressions of the mass-luminosity relation given in Delfosse et al. (2000). Against this paper sample, both expressions given in B05 perform equally, with B05(2) having a marginally higher dispersion. In the remaining of this paper we therefore elude B05(2).

4.2. Calibration of Johnson & Apps (2009)

Since our first attempt, further works have been proposed to improve on the metallicity calibration. Notably, Johnson & Apps (2009) have argued that M dwarfs should have the same metallicity as FGK stars and chose accordingly to fix their mean metallicity to the solar-neighborhood value (-0.05 dex). From a volume-limited sample of FGK dwarfs from the SPOCS sample (Valenti & Fischer 2005), they next determined a sequence representative of the average M dwarf in the $\{(V-K)-M_K\}$ color-magnitude diagram proposed by Bonfils et al. (2005). Then, they modeled the metallicity as the linear distance to that main sequence along $(V-K)$ (verify if it is V-K). To calibrate that scale, they used the metallicity of 6 metal-rich M dwarfs with values known from FGK primary components.

Fixing the metallicity of M dwarfs is a strong assumption that JA09 have motivated with two lines of arguments. Firstly, they presented [Fe/H] measurements for

[2] Mistakenly quoted to be a 0.09 dex difference in Johnson & Apps (2009)

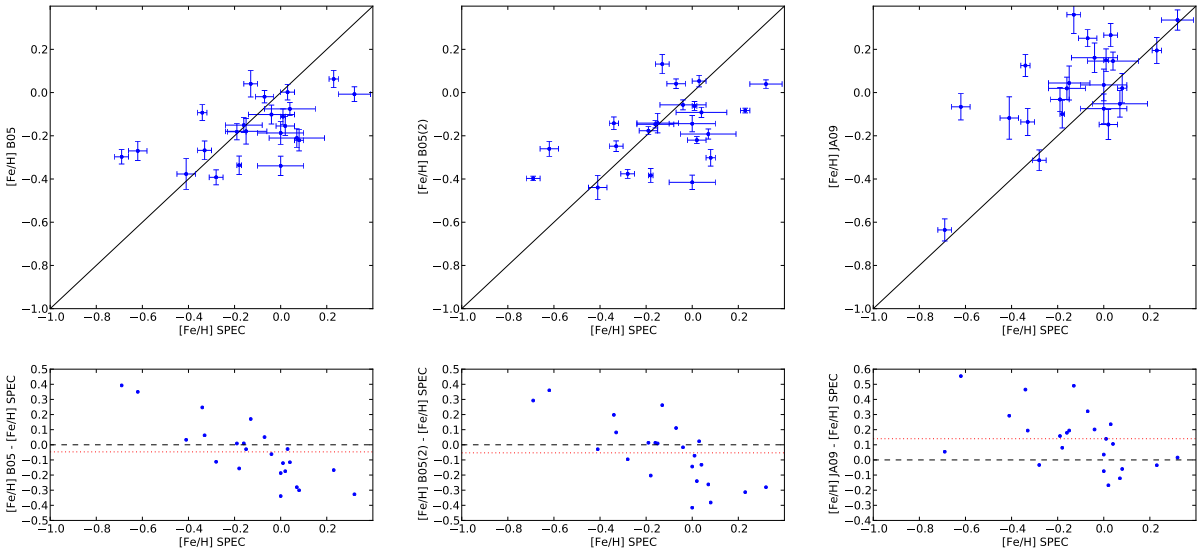

(a) B05 Calibration (b) B05(2) Calibration (c) JA09 Calibration

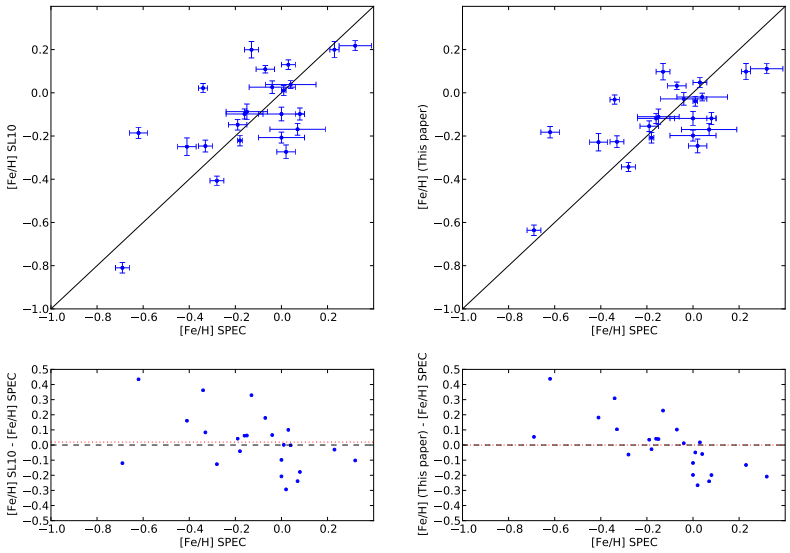

(d) SL10 Calibration (e) This paper

Fig. 1. [Fe/H] of the calibrations versus the spectroscopic metallicity. The tested calibrations are from Bonfils et al. (2005) (a and b), Johnson & Apps (2009) (c), and Schlaufman & Laughlin (2010) (d). The (e) panel depicts the update we did of the calibration of Schlaufman & Laughlin (2010) using the sample of this paper. The blue dots with error bars represent the data points. The black line depicts a one to one relationship. The metallicity difference between the values of the calibrations and the spectroscopic measurements is shown below each [Fe/H]-[Fe/H] plot. The black dashed line is the zero point of the difference, and the red dotted line represents the average of the metallicity difference.

109 G0-K2 stars that span effective temperatures from 4900 to 5900 K. They measured a weak Pearson correlation coefficient and concluded that, because no metallicity gradient is seen for this temperature range, no metallicity difference is to be expected for the cooler M dwarfs. We note, however, that when we did a linear fit to this data set ([Fe/H] $= 9.74 \times 10^{-5}.(T_{\rm eff} - 5777) - 0.04$) we found that any extrapolation to the cooler M dwarfs (2700<Teff<3750, from M7 to M0 spectral type) actually allows for a wide range of metallicities ($-0.32 <$ [Fe/H] < -0.22), that are values even lower than the [Fe/H] difference seen in B05. Secondly, they measured a large (0.32 dex) difference between B05 calibration and the primary-measured values for the 6 chosen metal-rich M dwarfs. This robustly points for a systematic offset in B05 calibra-

Table 2. Comparison of the offset, rms, residual mean square (RMS_P), and adjusted square of the multiple correlation coefficient (R^2_{ap}) of the calibrations of Bonfils et al. (2005), Casagrande et al. (2008), Johnson & Apps (2009), and Schlaufman & Laughlin (2010) applied to our data. The"This paper" calibration is a update to the Schlaufman & Laughlin (2010) calibration using the sample of this paper.

Calibration Source + equation	offset [dex]	rms [dex]	RMS_P [dex]	R^2_{ap}
B05 : $[Fe/H] = 0.196 - 1.527M_K + 0.091M_K^2 + 1.886(V-K) - 0.142(V-K)^2$	-0.05 ± 0.04	0.20 ± 0.02	0.04 ± 0.01	0.32 ± 0.22
B05(2) : $[Fe/H] = -0.149 - 6.508\Delta M, \Delta M = Mass_V - Mass_K$	-0.05 ± 0.04	0.21 ± 0.02	0.05 ± 0.01	0.22 ± 0.34
JA09 : $[Fe/H] = 0.56\Delta M_K - 0.05, \Delta M_K = MS - M_K$	0.14 ± 0.04	0.24 ± 0.04	0.06 ± 0.02	0.06 ± 0.49
SL10 : $[Fe/H] = 0.79\Delta(V-K) - 0.17, \Delta(V-K) = (V-K)_{obs} - (V-K)_{fit}$	0.02 ± 0.04	0.19 ± 0.03	0.03 ± 0.01	0.42 ± 0.28
This paper : $[Fe/H] = 0.595\Delta(V-K) - 0.158$	0.00 ± 0.04	0.17 ± 0.03	0.03 ± 0.01	0.44 ± 0.23

Table 3. Metallicity values from spectroscopy and for the calibrations of Bonfils et al. (2005), Casagrande et al. (2008), Johnson & Apps (2009), and Schlaufman & Laughlin (2010). The "This paper" column represents the [Fe/H] values of the new fit based on the Schlaufman & Laughlin (2010) calibration.

Primary	Secondary	[Fe/H] [dex]					
		Spectroscopic	B05	B05(2)	JA09	SL10	This paper
Gl53.1A	Gl53.1B	0.07	-0.21	-0.19	-0.05	-0.17	-0.17
Gl56.3A	Gl56.3B	0.00	-0.34	-0.42	-0.07	-0.21	-0.20
Gl81.1A	Gl81.1B	0.08	-0.22	-0.30	0.02	-0.10	-0.12
Gl100A	Gl100C	-0.28	-0.39	-0.38	-0.31	-0.41	-0.34
Gl105A	Gl105B	-0.19	-0.18	-0.18	-0.03	-0.15	-0.15
Gl140.1A	Gl140.1B	-0.41	-0.38	-0.44	-0.12	-0.25	-0.23
Gl157A	Gl157B	-0.13	0.04	0.13	0.36	0.20	0.10
Gl173.1A	Gl173.1B	-0.33	-0.27	-0.25	-0.14	-0.25	-0.23
Gl211	Gl212	0.04	-0.08	-0.09	0.15	0.04	-0.02
Gl231.1A	Gl231.1B	0.01	-0.11	-0.06	0.15	0.01	-0.04
Gl250A	Gl250B	-0.15	-0.18	-0.14	0.04	-0.09	-0.11
Gl297.2A	Gl297.2B	0.03	0.00	0.05	0.27	0.13	0.05
Gl324A	Gl324B	0.32	-0.01	0.04	0.34	0.22	0.11
Gl559A	Gl551	0.23	0.06	-0.08	0.19	0.20	0.10
Gl611A	Gl611B	-0.69	-0.30	-0.40	-0.64	-0.81	-0.64
Gl653	Gl654	-0.62	-0.27	-0.26	-0.07	-0.19	-0.18
Gl666A	Gl666B	-0.34	-0.09	-0.14	0.12	0.02	-0.03
Gl783.2A	Gl783.2B	-0.16	-0.15	-0.15	0.02	-0.10	-0.12
Gl797A	Gl797B	-0.07	-0.02	0.04	0.25	0.11	0.03
GJ3091A	GJ3092B	0.02	-0.15	-0.22	-0.15	-0.27	-0.25
GJ3194A	GJ3195B	0.00	-0.19	-0.14	0.04	-0.10	-0.12
GJ3627A	GJ3628B	-0.04	-0.10	-0.06	0.16	0.03	-0.03
NLTT34353	NLTT34357	-0.18	-0.34	-0.38	-0.10	-0.22	-0.21

tion, at least for the metal-rich part, but did not anchor the mean metallicity of M dwarfs.

In the high-metallicity range, where JA09 calibrators were chosen, the calibration matches well the metallicities of our sample. With decreasing metallicity JA09 calibration however gives too metal rich values (as already pointed out by SL10, see below). Notably, we measure a global offset of $+0.14 \pm 0.04$ dex and a dispersion of 0.23 ± 0.04.

4.3. Calibration of Schlaufman & Laughlin (2010)

Following on B05 and JA09 works, Schlaufman & Laughlin (2010) improved on our comprehension of M dwarf metallicity and its calibration.

First, they have shown that, for M dwarfs and FGK stars to share the same mean metallicity, a kinematic match is equally important as a volume-limited match for both samples. Indeed, the different kinematic populations of our Galaxy have significant different mean metallicities and the mean metallicity of small samples could fluctuate with the number of stars from each population. To overcome this statistical noise, they draw a volume-limited sample of F and G stars from the Geneva-Copenhagen Survey that matches kinematically the volume limited sample of M dwarfs used by JA09. They found that the sample of FGK stars has a mean metallicity of $\simeq -0.14 \pm 0.06$ dex, which is 0.09 dex lower than the value adopted by JA09.

Second, they use Baraffe et al. (1998) models to compute [Fe/H] isocontours. They show that in a $\{(V-K)-M_K\}$ diagram, a change in [Fe/H] results essentially in a change in (V−K), and almost no change in M_K. The [Fe/H] is therefore better calibrated by (V−K) and

they propose the calibration should be based on a linear function of the (V−K) distance in a {(V−K)−M_K} diagram. To remain free of any assumption regarding the mean metallicity of M dwarfs, they kept the ordinate at the origin of the calibration as a free parameter.

We used the SL10 sample to measure its dispersion and obtained a value of 0.14 ± 0.02 dex. But against our test sample, we measure a higher value of 0.19 ± 0.03. The dispersion difference may be explained by a larger dispersion, in our sample, of the M_k vs $(V-K)$ relationship, that translates solely into a larger range of the metallicity, as the effective temperature range is approximately the same. To test this hypothesis we measured the dispersion of a sub-sample of 18 stars inside the metallicity range of the sample of SL10. We obtained a dispersion value of 0.15 ± 0.02 dex, very similar to the result obtained for the SL10 sample. This may mean that the dispersion of our sample has physical roots rather that being due to measurement uncertainties.

We also measure an offset of 0.02 ± 0.04 dex. Both offset and rms improved over B05 and JA10 calibrations.

4.4. Updating the Schlaufman & Laughlin (2010) calibration

We have established a new fit following the SL10 prescription, using the RMS_p free parameter $p = 2$ (see Section 3). The expression for the new metallicity calibration is

$$[Fe/H] = 0.57\Delta(V-K_s) - 0.17, \quad (3)$$
$$\Delta(V-K_s) = (V-K_s)_{obs} - (V-K_s)_{iso},$$

where $(V-K_s)_{obs}$ is the observed photometric difference between V- and K_s-band and $(V-K_s)_{iso}$ is a 5th order polinomial as a function of M_{K_s} that denotes the mean main sequence of the Solar neighborhood from the SPOCS catalog. This expression was taken from Schlaufman & Laughlin (2010) and was defined originally as M_k as a function of $(V-K_s)$ by Johnson & Apps (2009). It has the following coefficients in increasing order: $51.1413, -39.3756, 12.2862, -1.83916, 0.134266$, and -0.00382023.

From the results shown in Table 2, we can observe that there are no significant differences between this new fit and the original calibration. The rms of the new fit is tighter just by 0.02 dex (from 0.19 ± 0.03 to 0.17 ± 0.03 dex), and the offset is now 0.00 ± 0.04, as expected. The R^2_{ap} value are similar (0.42 ± 0.28 vs 0.44 ± 0.23) despite having big uncertainties, and the RMS_p value is the same as the SL10 calibration. This means that the calibration of SL10 is still valid using our new data.

The dispersion of the sample, seen in all the plots of Fig. 1 is much higher than the uncertainties of the measurements. This means that we are not limited by measurement uncertainties. If this was not the case the points would be much closer to the identity line.

We must note the possible existence of a trend with spectroscopic [Fe/H], having a negative slope, for the B05, B05(2), and the calibration presented in this paper. This may also be the case for the remaining calibrations, if we ignore the data point with the lowest value of [Fe/H]. The B05 and B05(2) calibrations also seem to overestimate the metallicity for spectroscopic [Fe/H] < -0.4. Regarding higher metallicities, above 0.2 dex, only the calibrations of JA09 and SL10 seem to accurately predict the spectroscopic metallicities: all the other calibrations underestimate the [Fe/H] value. We do not know the cause of the [Fe/H] trend, but this may mean that the current models are missing a higher order trend.

5. Conclusion

This paper review several photometric calibrations of M-dwarf metallicity. With a sample of M dwarfs selected for their precisely known metallicity (from the literature or newly measured), photometry and parallaxes, we have performed a comparative test of Bonfils et al. (2005), Johnson & Apps (2009), and Schlaufman & Laughlin (2010)'s metallicity scales. Over the course of this paper we adopt the expression proposed by Schlaufman & Laughlin (2010) and update the metallicity calibration with a new fit on our sample.

We based our test on a classic variance analysis and show that only a weak improvement has been done over time. More importantly, we show that a carefully selected sample does not show a significantly lower variance against the various calibrations. Actually, to affirm that we would need to quantify the expected improvement... This most probably means that the calibration performance is not limited by measurement uncertainties but is rather rooted to physical limitations. Although more observations are required to confirm the photometric calibration is intrinsically limited, such a result already call for alternative strategy to calibrate the metallicity of M dwarfs. An obvious one is to increase the spectral resolution of our observations to disentangle the spectral parts most sensitive to the metallicity from other spectral parts most sensitive to the temperature. This approach is already showing encouraging results, either at infra-red wavelength (Rojas-Ayala et al. 2010, , see Appendix 2), or in the visible (Neves et al. in prep.).

Acknowledgements. We would like to thank Luca Casagrande for kindly providing us the metallicities calculated from his calibration. We acknowledge the support by the European Research Council/European Community under the FP7 through Starting Grant agreement number 239953. NCS also acknowledges the support from Fundação para a Ciência e a Tecnologia (FCT) through program Ciência 2007 funded by FCT/MCTES (Portugal) and POPH/FSE (EC), and in the form of grant reference PTDC/CTE-AST/098528/2008. VN would also like to acknowledge the support from FCT in the form of the fellowship SFRH/BD/60688/2009.

References

Baraffe, I., Chabrier, G., Allard, F., & Hauschildt, P. H. 1998, A&A, 337, 403
Bessell, M. S. 1990, AAPS, 83, 357
Bessell, M. S. 1991, AJ, 101, 662
Blackwell, D. E. & Shallis, M. J. 1977, MNRAS, 180, 177
Bonfils, X., Delfosse, X., Udry, S., Forveille, T., & Naef, D. 2006, in Tenth Anniversary of 51 Peg-b: Status of and prospects for hot Jupiter studies, ed. L. Arnold, F. Bouchy, & C. Moutou, 111–118
Bonfils, X., Delfosse, X., Udry, S., et al. 2005, A&A, 442, 635
Bonfils, X., Mayor, M., Delfosse, X., et al. 2007, ArXiv e-prints, 704
Bouchy, F., Mayor, M., Lovis, C., et al. 2009, A&A, 496, 527
Bouchy, F. & The Sophie Team. 2006, in Tenth Anniversary of 51 Peg-b: Status of and prospects for hot Jupiter studies, ed. L. Arnold, F. Bouchy, & C. Moutou, 319–325
Caldwell, J. A. R., Spencer Jones, J. H., & Menzies, J. W. 1984, MNRAS, 209, 51
Casagrande, L., Flynn, C., & Bessell, M. 2008, MNRAS, 389, 585
Casagrande, L., Portinari, L., & Flynn, C. 2006, MNRAS, 373, 13
Chabrier, G. & Baraffe, I. 2000, ARAA, 38, 337
Chanamé, J. & Gould, A. 2004, ApJ, 601, 289
Dahn, C. C., Harrington, R. S., Kallarakal, V. V., et al. 1988, AJ, 95, 237
Dahn, C. C., Harrington, R. S., Riepe, B. Y., et al. 1982, AJ, 87, 419
Dawson, P. C. & Forbes, D. 1992, AJ, 103, 2063
Delfosse, X., Forveille, T., Ségransan, D., et al. 2000, A&A, 364, 217
Eggen, O. J. 1976, ApJS, 30, 351
Eggen, O. J. 1979, ApJS, 39, 89
ESA. 1997, The Hipparcos and Tycho Catalogues
Fischer, D. A. & Valenti, J. 2005, ApJ, 622, 1102
Gliese, W. & Jahreiß, H. 1991, Preliminary Version of the Third Catalogue of Nearby Stars, Tech. rep.
Gonzalez, G. 1997, MNRAS, 285, 403
Gould, A. & Chanamé, J. 2004, ApJS, 150, 455
Hocking, R. R. 1976, Biometrics, 32, 1
Johnson, J. A. & Apps, K. 2009, ApJ, 699, 933
Kaufer, A. & Pasquini, L. 1998, in Society of Photo-Optical Instrumentation Engineers (SPIE) Conference Series, Vol. 3355, Society of Photo-Optical Instrumentation Engineers (SPIE) Conference Series, ed. S. D'Odorico, 844–854
Koen, C., Kilkenny, D., van Wyk, F., Cooper, D., & Marang, F. 2002, MNRAS, 334, 20
Kurucz, R. 1993, ATLAS9 Stellar Atmosphere Programs and 2 km/s grid. Kurucz CD-ROM No. 13. Cambridge, Mass.: Smithsonian Astrophysical Observatory, 1993., 13
Laing, J. D. 1989, South African Astronomical Observatory Circular, 13, 29
Leggett, S. K. 1992, ApJS, 82, 351
Mayor, M., Bonfils, X., Forveille, T., et al. 2009, A&A, 507, 487
Mermilliod, J., Mermilliod, M., & Hauck, B. 1997, A&AS, 124, 349
Pesch, P. 1982, PASP, 94, 345
Poveda, A., Herrera, M. A., Allen, C., Cordero, G., & Lavalley, C. 1994, Rev. Mexicana Astron. Astrofis., 28, 43
Queloz, D., Mayor, M., Weber, L., et al. 2000, A&A, 354, 99
Reid, I. N., Cruz, K. L., Allen, P., et al. 2004, AJ, 128, 463
Rojas-Ayala, B., Covey, K. R., Muirhead, P. S., & Lloyd, J. P. 2010, ApJ, 720, L113
Ryan, S. G. 1989, AJ, 98, 1693
Santos, N. C., Israelian, G., & Mayor, M. 2001, A&A, 373, 1019
Santos, N. C., Israelian, G., & Mayor, M. 2004, A&A, 415, 1153
Santos, N. C., Mayor, M., Naef, D., et al. 2002, A&A, 392, 215
Schlaufman, K. C. & Laughlin, G. 2010, ArXiv e-prints
Sinachopoulos, D. & van Dessel, E. L. 1996, AAPS, 119, 483
Skrutskie, M. F., Cutri, R. M., Stiening, R., et al. 2006, AJ, 131, 1163
Sneden, C. 1973, Ph.D. Thesis, Univ. of Texas
Sousa, S. G., Santos, N. C., Israelian, G., Mayor, M., & Monteiro, M. J. P. F. G. 2007, A&A, in press
Sousa, S. G., Santos, N. C., Mayor, M., et al. 2008, A&A, 487, 373
Udry, S., Bonfils, X., Delfosse, X., et al. 2007, A&A, 469, L43
Udry, S. & Santos, N. 2007, ARAA, 45, 397
Upgren, A. R. 1974, PASP, 86, 294
Valenti, J. A. & Fischer, D. A. 2005, VizieR Online Data Catalog, 215, 90141
van Leeuwen, F. 2007, A&A, 474, 653
Weis, E. W. 1988, AJ, 96, 1710
Weis, E. W. 1993, AJ, 105, 1962
Weis, E. W. 1996, AJ, 112, 2300
Weistrop, D. 1975, PASP, 87, 367
Weistrop, D. 1977, ApJ, 215, 845
Weistrop, D. 1981, AJ, 86, 1220
Woolf, V. M. & Wallerstein, G. 2005, MNRAS, 356, 963
Woolf, V. M. & Wallerstein, G. 2006, PASP, 118, 218

Appendix A: Other methods & sample table

A.1. Calibration of Casagrande et al. (2008)

In section 4 we describe in detail the photometric metallicity calibrations. A completely different technique was devised by Casagrande et al. (2008) based on his previous study of FGK stars using the infrared flux method

Table A.1. Metallicity values from spectroscopy and obtained using the method of Casagrande et al. (2008) (C08 in this Table).

Primary	Secondary	[Fe/H] [dex]	
		Spectroscopic	C08
Gl53.1A	Gl53.1B	0.07	-0.07
Gl56.3A	Gl56.3B	0.00	-0.21
Gl81.1A	Gl81.1B	0.08	-0.08
Gl100A	Gl100C	-0.28	-0.10
Gl105A	Gl105B	-0.19	-0.30
Gl140.1A	Gl140.1B	-0.41	-0.30
Gl157A	Gl157B	-0.13	-0.10
Gl173.1A	Gl173.1B	-0.33	-0.20
Gl211	Gl212	0.04	-0.21
Gl231.1A	Gl231.1B	0.01	-0.28
Gl250A	Gl250B	-0.15	-
Gl297.2A	Gl297.2B	0.03	0.00
Gl324A	Gl324B	0.32	-0.20
Gl559A	Gl551	0.23	-
Gl611A	Gl611B	-0.69	-0.40
Gl653	Gl654	-0.62	-0.30
Gl666A	Gl666B	-0.34	-
Gl783.2A	Gl783.2B	-0.16	-0.30
Gl797A	Gl797B	-0.07	-0.90
GJ3091A	GJ3092B	0.02	-0.30
GJ3194A	GJ3195B	0.00	-0.60
GJ3627A	GJ3628B	-0.04	-0.20
NLTT34353	NLTT34357	-0.18	0.19

Table A.2. Offset, rms, residual mean square (RMS_P), and adjusted square of the multiple correlation coefficient (R^2_{ap}) of the [Fe/H] values obtained using the Casagrande et al. (2008) method.

offset [dex]	rms [dex]	RMS_P [dex]	R^2_{ap}
-0.12 ± 0.07	0.32 ± 0.06	0.11 ± 0.04	-1.09 ± 1.47

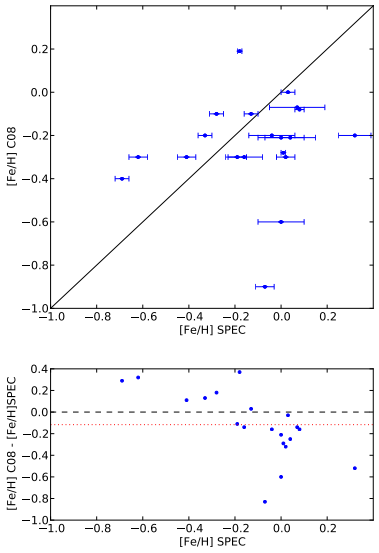

Fig. A.1. [Fe/H] obtained with the Casagrande et al. (2008) method versus the spectroscopic metallicity. The blue dots with error bars represent the data points. The black line depicts a one to one relationship. The metallicity difference between the values of the calibrations and the spectroscopic measurements is shown below each [Fe/H]-[Fe/H] plot. The black dashed line is the zero point of the difference, and the red dotted line represents the average of the metallicity difference.

(Casagrande et al. 2006) to determine effective temperatures and metallicities. The infrared flux method is a technique that uses multiple photometry bands to derive effective temperatures, bolometric luminosities, and angular diameters of the star. The basic idea of IRFM (Blackwell & Shallis 1977) is to compare the ratio between the bolometric flux and the infrared monochromatic flux, both measured at Earth, to the ratio between the surface bolometric flux ($\propto \sigma Teff^4$) and the surface infrared monochromatic flux of the star. In order to adapt this method to M dwarfs, optical bands were added, creating the so-called MOITE, Multiple Optical and Infrared TEchnique. This method provides very sensitive indicators of both temperature and metallicity, with the proposed effective temperature scale extending down to 2100-2200 K, into the L-dwarf limit, being supported by interferometric angular diameters above $\sim$ 3000K. The method followed by Casagrande et al. (2008) to recover the metallicities starts by obtaining the effective temperature for each colour band ($V(RI)_C JHK_S$) of a given star, assigning at each time a trial metallicity, from -2.1 to 0.4 dex, in steps of 0.1 dex. The correct value of the metallicity is found when the scatter among the six trial effective temperatures is at a minimum.

The total uncertainty for the metallicity is estimated to be between 0.2 and 0.3 dex.

We could not directly test the Casagrande et al. (2008) approach, because there is no published calibration available. However, we used the [Fe/H] values provided by Luca Casagrande, and shown in TableA.1 to test his method. Following Fig. A.1 and Table A.2, we can observe that the Casagrande et al. (2008) method has a higher rms, RMS_p and R^2_{ap} values when compared to the tested calibrations. The negative R^2_{ap} value means that this model is increasing the variance when compared to a constant model.

A.2. Calibration of Rojas-Ayala et al. (2010)

Rojas-Ayala et al. (2010) recently released a new paper describing a novel and very precise technique that allows an easier observation of M dwarfs. Their technique is based on the calculation of spectral indices via direct spectral analysis of moderate ($R \sim 2700$) near infrared spectra (K band), and has the advantage of not depending on V magnitudes nor parallaxes, allowing the study of fainter (or/and farther) stars. They analysed 17 M dwarfs secondaries with a FGK primary, that served also as metallicity

calibrators, and measured the equivalent widths of the NaI doublet (2.206 and 2.209 μm), and the CaI triplet (2.261, 2.263 and 2.265 μm). With these measurements and a water absorption spectral index sensitive to stellar temperatures, they constructed a metallicity scale with an adjusted multiple correlation coefficient greater than the one of Schlaufman & Laughlin (2010) ($R^2_{ap} = 0.63$), and also with a tighter RMS_p of 0.02 when compared to other studies (0.05, 0.04 and 0.02 for Bonfils et al. (2005), Johnson & Apps (2009), and Schlaufman & Laughlin (2010) respectively). The metallicity range of the calibration is between -0.5 and +0.5 dex, with an estimated uncertainty of $\pm$0.15 dex.

It would be very interesting to test the Rojas-Ayala et al. (2010) calibration. Unfortunately, we were not able to do it because we lack the infrared spectra to measure the spectral indexes necessary for the calibration. We were able to do an external test, by comparing the measurements of the seven stars in common (Gl 212, Gl 231.1B, Gl 250B, Gl 324B, Gl611B, Gl783.2B, and Gl 797B with predicted [Fe/H] of 0.09, -0.05, -0.04, 0.30, -0.49, -0.19, and -0.06 dex respectively). We got a value of only 0.08 dex for the dispersion and a 0.04 dex offset between the spectroscopic measurements and Rojas-Ayala et al. (2010) predicted metallicities. These numbers have little significance, but they may give a hint that the calibration is compatible with the spectroscopic measurements. With this external test, we cannot confirm or deny if this calibration is better than the one of Schlaufman & Laughlin (2010). However, the results suggests that this calibration should be properly tested in the future.

Table A.3. Sample of wide binaries with a FGK primary and a M dwarf secondary. The first and third columns display, respectively, the primary and the secondary stars, along with their respective spectral type (columns two and four). The fifth column depicts the parallaxes of the primary with its associated errors. The sixth column describes the metallicity values and its respective errors. From the seventh to the twelveth column, the $V(RI)_C JHK_S$ photometry is shown, as well as its associated errors. In the last two columns the sources for [Fe/H] and for the photometry are exhibited.

Primary	Sp.T.	Secondary	Sp.T.	π [mas]	[Fe/H] [dex]	V [mag]	R [mag]	I [mag]	J [mag]	H [mag]	K_s [mag]	[Fe/H] source	V/RI/JHK source
Gl53.1A	K4	Gl53.1B	M3	48.20 ± 1.06	0.07 ± 0.12	13.60 ± 0.02	12.48 ± 0.05	11.01 ± 0.05	9.533 ± 0.039	8.927 ± 0.023	8.673 ± 0.024	B05	W93/W93/2MASS
Gl56.3A	K1	Gl56.3B	K7	37.75 ± 0.95	0.00 ± 0.10	10.70 ± 0.02	9.84 ± 0.03	9.01 ± 0.03	8.012 ± 0.021	7.369 ± 0.029	7.190 ± 0.020	COR	B90/B90/2MASS
Gl81.1A	G9	Gl81.1B	K7	30.44 ± 0.60	0.08 ± 0.02	11.20 ± 0.01	10.30 ± 0.01	9.41 ± 0.01	8.413 ± 0.023	7.763 ± 0.021	7.597 ± 0.027	S08	C84/C84/2MASS
Gl100	K4.5	Gl100C	M2.5	51.16 ± 1.33	-0.27 ± 0.04	12.85 ± 0.01	11.79 ± 0.01	10.43 ± 0.01	9.181 ± 0.027	8.571 ± 0.029	8.347 ± 0.021	NEW	C84/C84/2MASS
Gl105A	K3	Gl105B	M4	139.27 ± 0.45	-0.17 ± 0.03	11.66 ± 0.02	10.45 ± 0.05	8.87 ± 0.05	7.333 ± 0.018	6.793 ± 0.038	6.574 ± 0.020	NEW	W93/W93/2MASS
Gl140.1A	K3.5	Gl140.1B	K8	51.95 ± 1.16	-0.41 ± 0.04	10.17 ± 0.01	-	-	7.436 ± 0.023	6.828 ± 0.023	6.620 ± 0.040	S08	S96/-/2MASS
Gl157A	K4	Gl157B	M2	64.40 ± 1.06	-0.13 ± 0.03	11.61 ± 0.03	-	-	7.773 ± 0.024	7.162 ± 0.033	6.927 ± 0.031	NEW	U74/-/2MASS
Gl173.1A	K3	Gl173.1B	M3	32.69 ± 1.51	-0.33 ± 0.03	14.19 ± 0.02	13.05 ± 0.05	11.65 ± 0.05	10.263 ± 0.022	9.715 ± 0.028	9.421 ± 0.024	NEW	W93/W93/2MASS
Gl211	K1	Gl212	M0	81.44 ± 0.54	0.04 ± 0.11	09.76 ± 0.01	8.81 ± 0.05	7.76 ± 0.05	6.586 ± 0.021	5.963 ± 0.016	5.759 ± 0.016	B05	HIP/W93/2MASS
Gl231.1A	G0	Gl231.1B	M3.5	51.95 ± 0.40	0.01 ± 0.01	13.27 ± 0.02	12.15 ± 0.05	10.62 ± 0.05	9.088 ± 0.023	8.559 ± 0.042	8.267 ± 0.018	NEW	WT81/WT81/2MASS
Gl250A	K3	Gl250B	M2	114.94 ± 0.86	-0.15 ± 0.09	10.08 ± 0.01	9.04 ± 0.01	7.80 ± 0.01	6.579 ± 0.034	5.976 ± 0.055	5.723 ± 0.036	B05	L89/L89/2MASS
Gl297.2A	F6.5	Gl297.2B	M2	44.68 ± 0.30	0.03 ± 0.03	11.80 ± 0.02	-	-	8.276 ± 0.019	7.672 ± 0.027	7.418 ± 0.016	NEW	R04/-/2MASS
Gl324A	G8	Gl324B	M4	81.03 ± 0.75	0.32 ± 0.07	13.16 ± 0.01	11.94 ± 0.05	10.27 ± 0.05	8.560 ± 0.027	7.933 ± 0.040	7.666 ± 0.023	B05	D88/WT77/2MASS
Gl559A	G2	Gl551	M6	772.33 ± 2.42	0.21 ± 0.03	11.05 ± 0.02	9.43 ± 0.03	7.43 ± 0.03	5.357 ± 0.023	4.835 ± 0.057	4.31 ± 0.03	NEW	B90/B90/B91
Gl611A	G8	Gl611B	M4	68.87 ± 0.33	-0.69 ± 0.03	14.23 ± 0.02	13.00 ± 0.05	11.38 ± 0.05	9.903 ± 0.021	9.453 ± 0.021	9.159 ± 0.017	SPO	W96/W96/2MASS
Gl653	K5	Gl654	M2	93.40 ± 0.94	-0.62 ± 0.04	10.07 ± 0.01	9.10 ± 0.01	7.95 ± 0.01	6.780 ± 0.029	6.193 ± 0.021	5.975 ± 0.026	S08	K02/K02/2MASS
Gl666A	G8	Gl666B	M0	113.61 ± 0.69	−0.34 ± 0.02	08.70 ± 0.01	-	-	–	5.112 ± 0.023	4.856 ± 0.020	NEW	E79/-/2MASS
Gl783.2A	K1	Gl783.2B	M4	49.04 ± 0.65	-0.16 ± 0.08	14.06 ± 0.02	12.81 ± 0.03	11.20 ± 0.03	9.627 ± 0.018	9.108 ± 0.015	8.883 ± 0.018	B05	D92/D92/2MASS
Gl797A	G5	Gl797B	M2.5	47.65 ± 0.76	-0.07 ± 0.04	11.87 ± 0.01	-	-	8.160 ± 0.020	7.645 ± 0.023	7.416 ± 0.016	B05	D82/-/2MASS
GJ3091A	K2	GJ3092B	M	33.83 ± 1.00	0.02 ± 0.04	15.64 ± 0.03	13.81 ± 0.05	11.97 ± 0.05	11.092 ± 0.023	10.540 ± 0.026	10.266 ± 0.021	S08	P82 / E76 / 2MASS
GJ3194A	G4	GJ3195B	M3	41.27 ± 0.58	0.00 ± 0.10	12.55 ± 0.02	11.49 ± 0.05	10.15 ± 0.05	8.877 ± 0.021	8.328 ± 0.023	8.103 ± 0.029	SOP	W96 / W96 / 2MASS
GJ3627A	G5	GJ3628B	M3.5	38.58 ± 2.17	-0.04 ± 0.10	14.10 ± 0.03	12.88 ± 0.05	11.31 ± 0.05	9.828 ± 0.022	9.247 ± 0.021	9.015 ± 0.018	SOP	W88 / W88 / 2MASS
NLTT34353	G5	NLTT34357	K7	20.73 ± 1.05	-0.18 ± 0.01	12.41 ± 0.02	11.51 ± 0.03	10.59 ± 0.03	9.595 ± 0.026	8.910 ± 0.026	8.734 ± 0.019	NEW	R89 / R89 / 2MASS

References. [B05] Bonfils et al. (2005); [COR] CCF [Fe/H] taken from spectra of the CORALIE Spectrograph; [S08] Sousa et al. (2008); [NEW] This paper; [SPO] Valenti & Fischer (2005); [SOP] CCF [Fe/H] taken from spectra of the SOPHIE Spectrograph (Bouchy & The Sophie Team 2006); [W93] Weis (1993); [B90] Bessell (1990); [C84] Caldwell et al. (1984); [S96] Sinachopoulos & van Dessel (1996); [U74] Upgren (1974); [HIP] ESA (1997); [W81] Weistrop (1981); [L89] Laing (1989); [R04] Reid et al. (2004); [D88] Dahn et al. (1988); [W77] Weistrop (1977); [W96] Weis (1996); [K02] Koen et al. (2002); [E79] - Eggen (1979) [D92] - Dawson & Forbes (1992); [D82] Dahn et al. (1982); [P82] Pesch (1982); [E76] Eggen (1976); [W88] Weis (1988); [R89] Ryan (1989); [B91] Bessell (1991); [2MASS] Skrutskie et al. (2006).